

Cosmic Magnetic Fields and Their Influence on Ultra-High Energy Cosmic Ray Propagation

Günter Sigl^a Francesco Miniati, Torsten A. Enßlin^b

^a GReCO, Institut d’Astrophysique de Paris, C.N.R.S., 98 bis boulevard Arago, F-75014 Paris, France
 Fédération de Recherche Astroparticule et Cosmologie, Université Paris 7, 2 place Jussieu, 75251 Paris Cedex 05, France

^b Max-Planck Institut für Astrophysik, Karl-Schwarzschild-Str. 1, 85741 Garching, Germany

We discuss the influence of large scale cosmic magnetic fields on the propagation of hadronic cosmic rays above 10^{19} eV based on large scale structure simulations. Our simulations suggest that rather substantial deflection up to several tens of degrees at 10^{20} eV are possible for nucleon primaries. Further, spectra and composition of cosmic rays from individual sources can depend on magnetic fields surrounding these sources in intrinsically unpredictable ways. This is true even if deflection from such individual sources is small. We conclude that the influence of large scale cosmic magnetic fields on ultra-high energy cosmic ray propagation is currently hard to quantify. We discuss possible reasons for discrepant results of simulations by Dolag et al. which predict deflections of at most a few degrees for nucleons. We finally point out that even in these latter simulations a possible heavy component would in general suffer substantial deflection.

1. Introduction

The origin of ultra-high energy cosmic rays (UHECR) above 10^{19} eV ($= 10$ EeV) has been challenging physicists for many years [1,2]. Several next-generation experiments, most notably the Pierre Auger experiment now under construction [3] and the EUSO project [4] are now trying to solve this mystery.

Although statistically meaningful information about the UHECR energy spectrum and arrival direction distribution has been accumulated, no conclusive picture for the nature and distribution of the sources emerges naturally from the data. There is on the one hand the approximate isotropic arrival direction distribution [5] which indicates that we are observing a large number of weak or distant sources. On the other hand, there are also indications which point more towards a small number of local and therefore bright sources, especially at the highest energies: First, the AGASA ground array claims statistically significant multi-plets of events from the same directions within a few degrees [6,5], although this is

controversial [7] and has not been seen so far by the fluorescence experiment HiRes [8]. The spectrum of this clustered component is $\propto E^{-1.8}$ and thus much harder than the total spectrum [6]. Second, nucleons above $\simeq 70$ EeV suffer heavy energy losses due to photo-pion production on the cosmic microwave background — the Greisen-Zatsepin-Kuzmin (GZK) effect [9] — which limits the distance to possible sources to less than $\simeq 100$ Mpc [10]. Heavy nuclei at these energies are photo-disintegrated in the cosmic microwave background within a few Mpc [11]. For a uniform source distribution this would predict a “GZK cutoff”, a drop in the spectrum. However, the existence of this “cutoff” is not established yet from the observations [12].

The picture is further complicated by the likely presence of large scale extra-galactic magnetic fields (EGMF) that will lead to deflection of any charged UHECR component. Magnetic fields are ubiquitous in the Universe, although their origin is still unclear [13]. Magnetic fields in galaxies are observed with typical strengths of a few micro Gauss. In addition there is some evidence

for fields correlated with larger structures such as galaxy clusters [14]. Magnetic fields as strong as $\simeq 1\mu G$ in sheets and filaments of the large scale galaxy distribution, such as in our Local Supercluster, are compatible with existing upper limits on Faraday rotation [14,15]. It is also possible that fossil cocoons of former radio galaxies, so called radio ghosts, contribute significantly to the isotropization of UHECR arrival directions [16].

To get an impression of typical deflection angles one can characterize the EGMF by its r.m.s. strength B and a coherence length l_c . If we neglect energy loss processes for the moment, then the r.m.s. deflection angle over a distance $r \gtrsim l_c$ in such a field is $\theta(E, r) \simeq (2rl_c/9)^{1/2}/r_L$ [17], where the Larmor radius of a particle of charge Ze and energy E is $r_L \simeq E/(ZeB)$. In numbers this reads

$$\begin{aligned} \theta(E, r) \simeq & 0.8^\circ Z \left(\frac{E}{10^{20} \text{ eV}} \right)^{-1} \left(\frac{r}{10 \text{ Mpc}} \right)^{1/2} \\ & \times \left(\frac{l_c}{1 \text{ Mpc}} \right)^{1/2} \left(\frac{B}{10^{-9} \text{ G}} \right), \end{aligned} \quad (1)$$

for $r \gtrsim l_c$. This expression makes it immediately obvious that fields of fractions of micro Gauss lead to strong deflection even at the highest energies. This goes along with a time delay $\tau(E, r) \simeq r\theta(E, d)^2/4$, or

$$\begin{aligned} \tau(E, r) \simeq & 1.5 \times 10^3 \text{ yr} Z^2 \left(\frac{E}{10^{20} \text{ eV}} \right)^{-2} \\ & \times \left(\frac{r}{10 \text{ Mpc}} \right)^2 \left(\frac{l_c}{\text{Mpc}} \right) \left(\frac{B}{10^{-9} \text{ G}} \right)^2, \end{aligned} \quad (2)$$

which can be millions of years. A source visible in UHECR today could therefore be optically invisible since many models involving, for example, active galaxies as UHECR accelerators, predict variability on shorter time scales. Strong deflection also limits the distance r a UHECR of given energy can travel during its energy loss time, which sometimes is called a “magnetic horizon” [18,19]. For example, if energy losses are included, for a space-filling field $B \sim 1 \text{ nG}$ with $l_c = 1 \text{ Mpc}$ the propagation distance of UHECR above 10^{19} eV is limited to $\sim 400 \text{ Mpc}$ [18]. For fields $B \sim 0.1 \mu \text{G}$ the magnetic horizon would be only $\sim 20 \text{ Mpc}$ [19].

2. Numerical Simulations: Large Scale Structure

Quite a few simulations of the effect of extragalactic magnetic fields (EGMF) on UHECR exist in the literature, but usually idealizing assumptions concerning properties and distributions of sources or EGMF or both are made: In Refs. [20,21,22,18,23] sources and EGMF follow a pancake profile mimicking the local supergalactic plane. In other studies EGMF have been approximated in a number of fashions: as negligible [24,25], as stochastic with uniform statistical properties [26,27,28], or as organized in spatial cells with a given coherence length and a strength depending as a power law on the local density [29]. Recently, Ref. [16,30] have carried out the first attempts to simulate UHECR propagation in a realistically structured universe; additional, independent calculations have now followed [31]. So far all of these simulations have been limited to the case of nucleons.

In Ref. [30] the magnetized extragalactic environment used for UHECR propagation is produced by a simulation of the large scale structure of the Universe. The simulation was carried out within a computational box of $50 h^{-1} \text{ Mpc}$ length on a side, with normalized Hubble constant $h \equiv H_0/(100 \text{ km s}^{-1} \text{ Mpc}^{-1}) = 0.67$, and using a comoving grid of 512^3 zones and 256^3 dark matter particles. The EGMF was initialized to zero at simulation start and subsequently its seeds were generated at cosmic shocks through the Biermann battery mechanism [32]. Since cosmic shocks form primarily around collapsing structures including filaments, the above approach avoids generating EGMF in cosmic voids. In this particular case (more are explored, see below) the resulting magnetic fields in collapsed structures are rather extended, as can be seen in Fig. 1 (top panel), significantly more than in the case of a uniform initial seed field (Fig. 1 lower panel). The resulting EGMF has been shown to be compatible with existing Faraday rotation measures with lines of sight both through clusters and the diffuse intergalactic medium [15].

In Ref. [30] the following question was addressed: which observer positions, and source dis-

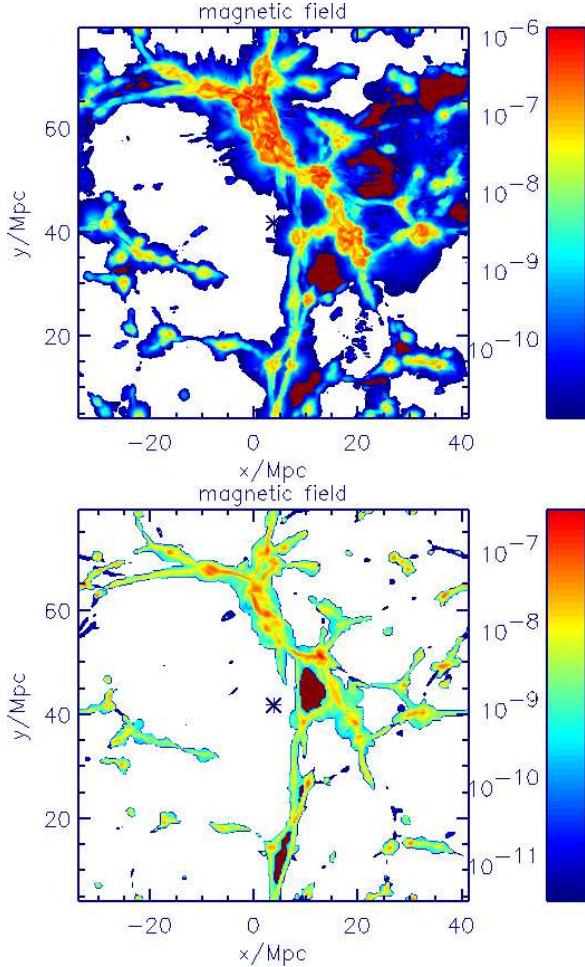


Figure 1. Log-scale two-dimensional cuts through magnetic field total strength in Gauss (color scale in Gauss) for two EGMF scenarios. In the upper panel seed fields were injected at shocks, as in the scenario studied in Ref. [30], whereas in the lower panel, an initial uniform seed field was assumed. In both cases the seeds are chosen such that the final fields are of order $\sim 1\mu\text{G}$ in a Coma-like cluster. For the latter case, fields in the voids were suppressed to minimize deflection. The observer is in the center of the figures and is marked by a star. The EGMF strength at the observer is $\simeq 10^{-11}\text{G}$ in the upper panel and ~ 0 in the lower panel. The roughly spherically magnetized region about 3 Mpc to the lower right of the observer in the upper panel was used to simulate UHECR fluxes from an individual source, see Sect. 3.

tributions and characteristics lead to UHECR distributions whose spherical multi-poles for $l \leq 10$ and auto-correlation at angles $\theta \lesssim 20^\circ$ are consistent with observations? It was found that (i) the observed large scale UHECR isotropy requires the neighborhood within a few Mpc of the observer is characterized by weak magnetic fields below $0.1\mu\text{G}$, and (ii) once that choice is made, current data do not strongly discriminate between uniform and structured source distributions and between negligible and considerable deflection. Nevertheless, current data moderately favor a scenario in which (iii) UHECR sources have a density $n_s \sim 10^{-5}\text{Mpc}^{-3}$ and follow the matter distribution and (iv) magnetic fields are relatively pervasive within the large scale structure, including filaments, and with a strength of order of a μG in galaxy clusters. A two-dimensional cut through the EGMF environment of the observer in a typical such scenario is shown in Fig. 1.

It was also studied in Ref. [30] how future data of considerably increased statistics can be used to learn more about EGMF and source characteristics. In particular, low auto-correlations at degree scales imply magnetized sources quite independent of other source characteristics such as their density. The source characteristics can only be estimated from the auto-correlations halfway reliably if magnetic fields have negligible impact on propagation. Otherwise, the images of sources immersed in considerable magnetic fields are smeared out, which also smears out the auto-correlation function over several degrees. For a sufficiently high source density, individual images can thus overlap and sensitivity to source density is consequently lost. The statistics expected from next generation experiments such as Pierre Auger [3] and EUSO [4] should be sufficient to test source magnetization by the auto-correlation function [30].

In Ref. [31] a constrained simulation which approximately reproduces the local universe on scales between a few Mpc and 115 Mpc from Earth was performed and the magnetic smoothed particle hydrodynamics technique was used to follow the EGMF evolution. The EGMF was seeded by a uniform seed field of maximal strength compatible with observed rotation measures in galaxy

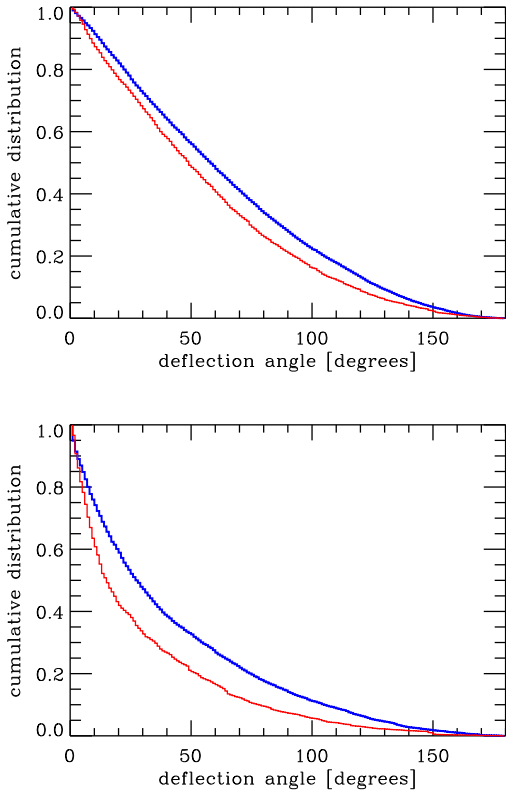


Figure 2. The cumulative distribution of deflection angles α with respect to the line of sight to the sources of cosmic rays above 4×10^{19} eV (upper panel) and above 10^{20} eV (lower panel). The blue (thick) and red (thin) curves showing larger and smaller deflections, respectively, are for the two EGMF scenarios from Fig. 1 upper and lower panel, respectively. The sources follow the baryon density and have average density $n_s = 2.4 \times 10^{-5} \text{ Mpc}^{-3}$. Shown are the averages over several realizations varying in the positions and luminosities Q_i of individual sources, the latter assumed to be distributed as $dn_s/dQ_i \propto Q_i^{-2.2}$ with $1 \leq Q_i \leq 100$ in arbitrary units.

clusters.

The questions considered in this work were somewhat different. In Ref. [31] deflections of UHECR above 4×10^{19} eV were computed as a function of the direction to their source which were assumed to be at cosmological distances. Specific source distributions were not considered. The deflections typically were found to be smaller than a few degrees.

Interestingly, however, there are considerable quantitative differences in the typical deflection angles predicted by the two EGMF models in Refs. [30,31]. These are *not* due to specific source distributions: In fact, for homogeneous source distributions, the average deflection angle for UHECR above 4×10^{19} eV obtained in Ref. [30] is $\simeq 61^\circ$ above 4×10^{19} eV and $\sim 33^\circ$ above 10^{20} eV, much larger than in Ref. [31].

In addition, even if the magnetic field strength is reduced by a factor 10 in the simulations in the environment of Fig. 1, upper panel, the average deflection angle is still $\sim 28^\circ$ above 4×10^{19} eV, and $\sim 10^\circ$ above 10^{20} eV. This non-linear behavior of deflection with field normalization is mostly due to the strongly non-homogeneous character of the EGMF.

Recently we have carried out a new simulation in which the initial magnetic seeds are provided by a uniform magnetic field (instead of the Biermann battery) to check how this different model affects our results. However, we find that typical deflection angles change at most by a factor of 2. This is demonstrated by Fig. 2 which compares deflection angle distributions for the two EGMF scenarios shown in Figs. 1 based on the Biermann battery model or uniform initial seeds, respectively. In both the above cases the magnetic fields in a Coma-like cluster at $z = 0$ were of order μG . Also, in the case of uniform initial fields we have further suppressed fields in the voids to minimize deflections.

Thus the residual differences in the predictions for the deflection angles of UHECR are probably due to the different numerical models for the magnetic fields. Numerical issues may play an important role because they affect the amplification and the topological structure of the magnetic fields, both of which are important for the nor-

malization procedure, see below. A few examples are provided in the following. The resolution in Ref. [30] is constant and in general better in filaments and voids but worse in the core of galaxy clusters than the (variable) resolution in Ref. [31]. Magnetohydrodynamic (MHD) codes are affected by numerical viscosity to a much larger extent than hydro codes; for this reason is it advantageous to evolve the magnetic field as a passive quantity because, while the amplification due to compression and stretching is fully accounted for, the additional dissipation introduced by the more complex MHD scheme is avoided. This is even more worrisome for the case of Ref. [31] where the numerical dissipation is not quantified. It is also worth noting that the algorithm employed in Ref. [31] does not guarantee a divergence-free magnetic field. While it is argued that in the high density regions (core of galaxy clusters) the variations of the magnetic fields on a scale of a few resolution elements are larger than the divergence-component, such conditions do not apply as easily in the low density, low resolution regions such as in filaments. Thus, one may wonder about the reliability of the numerical solution there.

In conclusion, while in both simulations the magnetic fields are normalized to (or reproduce) the same “observed” values in the core of rich clusters, their values in the filaments are substantially different. While in Ref. [30] the amplification in cluster cores may be underestimated, the magnetic fields in the filaments are not ruled out by available observational data [15]. On the other hand, there is some concern for the reliability of the numerical results of Ref. [31] in the low density regions, because numerical effects have not been quantified there.

As a result, the magnetic fields obtained in Ref. [30] are considerably more extended than the ones in Ref. [31]. This can be seen by comparing Fig. 3 with a similar plot in Ref. [33]: For the case shown in the upper panel of Fig. 3, about 10% of the volume is filled with fields stronger than 10 nano Gauss, and a fraction of 10^{-3} is filled by fields above a micro Gauss. Corresponding filling factors for these field strengths in case of Ref. [33] are $\lesssim 10^{-4}$ and $\lesssim 3 \times 10^{-6}$, respectively. This is the most likely reason for the much larger average

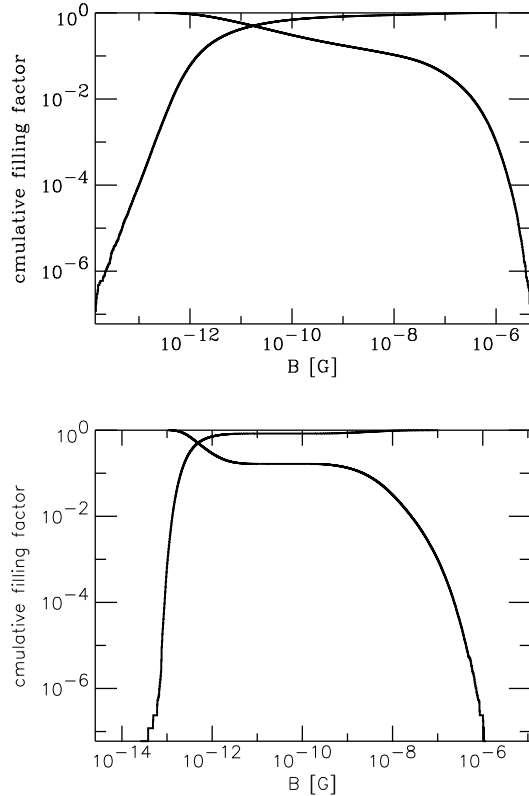


Figure 3. The cumulative filling factors for EGMF strength in the two simulations shown in Fig. 1 above (decreasing curve) and below (increasing curve) a given threshold, as a function of that threshold. Upper and lower panels correspond to the panels in Fig. 1.

deflections obtained in Ref. [30] as compared to the degree scale deflections discussed in Ref. [31].

Since very little is currently known about the properties of intergalactic magnetic fields, the only solid conclusion that can be drawn at this stage is that the effects of EGMF on UHECR propagation are currently rather uncertain.

Finally we note that these studies should be extended to include heavy nuclei [34] since there are indications that a fraction as large as 80% of iron nuclei may exist above 10^{19} eV [35]. Preliminary results [34] give deflections of $\sim 60^\circ$ above 10^{20} eV in our standard scenario shown in Figs. 1 and 3, upper panels. More importantly, even in the EGMF scenario of Ref. [31], deflections could be considerable and may not allow particle astronomy along many lines of sight: The distribution of deflection angles in Ref. [31] shows that deflections of protons above 4×10^{19} eV of $\gtrsim 1^\circ$ cover a considerable fraction of the sky. Suppression of deflection along typical lines of sight by small filling factors of deflectors is thus unimportant in this case. The deflection angle of any nucleus at a given energy passing through such areas will therefore be roughly proportional to its charge as long as energy loss lengths are larger than a few tens of Mpc [36]. Deflection angles of $\sim 20^\circ$ at $\sim 4 \times 10^{19}$ eV should thus be the rule for iron nuclei. In contrast to the contribution of our Galaxy to deflection which can be of comparable size but may be corrected for within sufficiently detailed models of the galactic field, the extra-galactic contribution would be stochastic. Statistical methods are therefore likely to be necessary to learn about UHECR source distributions and characteristics. In addition, should a substantial heavy composition be experimentally confirmed up to the highest energies, some sources would have to be surprisingly nearby, within a few Mpc, otherwise only low mass spallation products would survive propagation [37].

The putative clustered component of the UHECR flux whose fraction of the total flux seems to increase with energy [6] may play a key role in this context. It could be caused by discrete sources in directions with small deflection. Since, apart from energy losses, cosmic rays of same rigidity Z/A are deflected similarly by

cosmic magnetic fields, one may expect that the composition of the clustered component may become heavier with increasing energy. Indeed, in Ref. [38] it was speculated that the AGASA clusters may be consistent with consecutive He, Be-Mg, and Fe bumps.

3. Numerical Simulations: Discrete Sources

This brings us to the impact of EGMF on UHECR fluxes from discrete sources. In Ref. [39] we investigated the impact on cosmic ray observations above 10^{19} eV of Mpc-scale magnetic fields of $\sim 10^{-7}$ G strength surrounding UHECR sources. The likely case was assumed that magnetic fields within a few Mpc around Earth are insignificant. The trajectory simulations are based on the same large scale structure simulation as before, examples of whose EGMF distributions were shown in Figs. 1 and 3, upper panels. We find that such source fields can strongly modify spectra and composition at Earth, especially for nearby sources for which the fields can considerably increase propagation times relative to both energy loss and photo-disintegration time scales and to the undeflected propagation time: Eq. (2) shows qualitatively that time delays at $E \sim 10^{20}$ eV can easily reach $\sim 10^7$ years for fields $B \sim 10^{-7}$ G extended over a few Mpc. This is indeed larger than energy loss times $\sim 3 \times 10^6$ years and comparable to the straight line propagation time $\sim 10^7$ years. We found the following generic features:

We note in passing that spallation and pion production could be enhanced around powerful sources due to an increased infra-red background [40]. While we have not yet taken this into account in the present simulations, we expect this effect to be small compared to the EGMF effect.

The spectra are considerably hardened relative to the injection spectrum at energies below the usual GZK-like cutoff where energy loss distance and source distance become comparable. This is caused by an interplay between diffusion and energy loss: The flux of low energy particles is suppressed because diffusion spreads them out over a larger volume due to their much larger energy

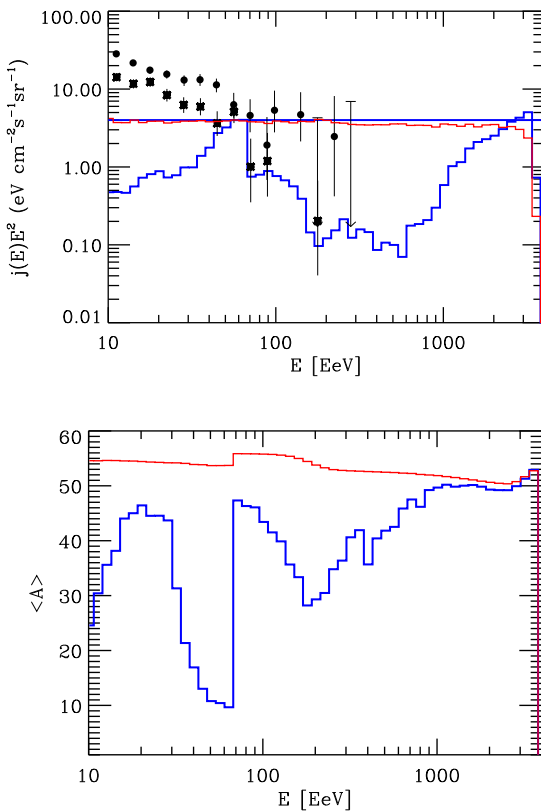


Figure 4. Upper panel: Steady state all-particle spectra predicted by a scenario with a source at 3.3 Mpc distance from Earth injecting iron primaries with a spectrum $\propto E^{-2.0}$ up to 4×10^{21} eV. The blue (thick) curves are for an EGMF of strength $\sim 10^{-7}$ G surrounding the source and the red (thin) curve is without EGMF. Shown for comparison are the solid angle integrated AGASA [41] (dots) and HiRes-I [42] (stars) data. The solid straight line marks the injection spectrum. All fluxes have been normalized at 60 EeV. Lower panel: The predicted composition in the same scenario.

loss times. This is in contrast to the case of uniformly distributed magnetic fields which in general lead to a steepening of the cosmic ray flux below the GZK cutoff. A hardened sub-GZK spectrum from individual sources would indeed be consistent with the hints of a hard clustered component in the AGASA data between 10^{19} eV and 10^{20} eV [6].

Furthermore, for a nucleus of atomic mass A as injected primary, due to the kinematics of the photo-disintegration reactions a nucleon peak appears at energy $\sim E_{\max}/A$, where E_{\max} is the maximal nucleus injection energy. This effect is the more prominent the harder the injection spectrum. We also found that the details of spectra and composition depend significantly on the unknown details of the magnetic fields and the position of the source therein and can thus not be predicted.

An example demonstrating these effects is shown in Fig. 4 where a source of iron nuclei at 3.3 Mpc distance to Earth is considered, once without any EGMF, and once with an EGMF concentrated around the source and reaching $\sim 10^{-7}$ G there. The observer is at the same position as indicated in Fig. 1 and the source is in the center of the roughly spherically magnetized region to the lower right of the observer in the upper panel of Fig. 1. The spectral modification for proton primaries (not shown) by the EGMF would be equally severe as in Fig. 4 [39].

Further cutoffs towards low energies can be induced if the source is active only since a time smaller than the typical delay time at this energy. Since the latter easily reaches $\sim 10^9$ years at 10^{19} eV in the scenario shown in Fig. 4, as can also be seen from Eq. (2), this is actually quite likely for active galactic nuclei which can have activity time scales below $\sim 10^8$ years. Obviously, the characteristics of such features also depend on unknown details of the source.

Our simulations finally show that even for iron primaries, extra-galactic magnetic fields from large scale structure simulations are not strong and extended enough to explain the observed large scale isotropy of UHECR arrival directions in terms of a single nearby source. This would require more homogeneous fields such as

in Ref. [43].

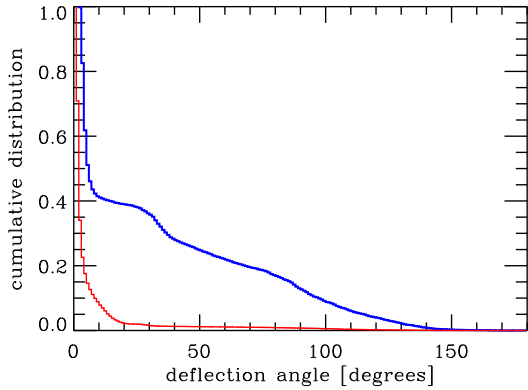


Figure 5. The cumulative distribution of arrival direction off-sets from the source direction for UHECR above 4×10^{19} eV in the scenario described in the text for iron primaries, corresponding to Fig. 4 (blue, thick curve) and proton primaries (red, thin curve).

Next generation experiments such as the Pierre Auger Observatories [3] and the EUSO project [4] will accumulate sufficient statistics to establish spectra and distributions of composition and arrival directions from individual sources. A potentially strong influence of magnetic fields surrounding individual sources should thus be kept in mind when interpreting data from these experiments. This is true even if UHECR arrive within a few degrees from the source position. As Fig. 5 shows [39], this is in fact the case for proton primaries in our example for a discrete source.

4. Conclusions

It thus seems evident that the influence of large scale cosmic magnetic fields on ultra-high energy cosmic ray propagation is currently hard to quantify and may not allow to do “particle astronomy” along most lines of sight, especially if a significant heavy nucleus component is present above

10^{19} eV. However, even in our simulations, there are lines of sight along which deflection is only a few degrees, at least for proton primaries. Such directions might still be suitable for “particle astronomy”.

Acknowledgments

GS thanks Antonio Insolia for inviting me to the CRIS meeting and for financial support.

REFERENCES

1. for recent reviews see P. Bhattacharjee and G. Sigl, *Phys. Rept.* **327**, 109 (2000) [arXiv:astro-ph/9811011]. J. W. Cronin, *Rev. Mod. Phys.* **71**, S165 (1999); M. Nagano and A. A. Watson, *Rev. Mod. Phys.* **72**, 689 (2000); A. V. Olinto, *Phys. Rept.* **333**, 329 (2000) [arXiv:astro-ph/0002006]; X. Bertou, M. Boratav and A. Letessier-Selvon, *Int. J. Mod. Phys. A* **15**, 2181 (2000) [arXiv:astro-ph/0001516]; G. Sigl, *Science* **291**, 73 (2001); F. W. Stecker, *J. Phys. G* **29**, R47 (2003) [arXiv:astro-ph/0309027].
2. “Physics and Astrophysics of Ultra High Energy Cosmic Rays”, Lecture Notes in Physics, **576** (Springer Verlag, 2001), eds. M. Lemoine, G. Sigl.
3. J. W. Cronin, *Nucl. Phys. Proc. Suppl.* **28B**, 213 (1992); The Pierre Auger Observatory Design Report (ed. 2), March 1997; see also <http://www.auger.org>.
4. See <http://www.euso-mission.org>.
5. W. S. Burgett and M. R. O’Malley, *Phys. Rev. D* **67**, 092002 (2003) [arXiv:hep-ph/0301001].
6. M. Teshima et al., *Proc. 28th International Cosmic Ray Conference*, Tsukuba, Japan, **1**, 437 (2003); see <http://www-rccn.icrr.u-tokyo.ac.jp/icrc2003/PROCEEDINGS/PROCEEDINGS.html>.
7. C. B. Finley and S. Westerhoff, *Astropart. Phys.* **21**, 359 (2004) [arXiv:astro-ph/0309159].
8. C. B. Finley et al., *Proc. 28th International Cosmic Ray Conference*, Tsukuba, Japan, **1**, 433 (2003); see <http://www-rccn.icrr.u-tokyo.ac.jp/icrc2003/PROCEEDINGS/PROCEEDINGS.html>.

9. K. Greisen, Phys. Rev. Lett. **16**, 748 (1966); G. T. Zatsepin and V. A. Kuzmin, JETP Lett. **4**, 78 (1966) [Pisma Zh. Eksp. Teor. Fiz. **4**, 114 (1966)].
10. F. W. Stecker, Phys. Rev. Lett. **21**, 1016 (1968).
11. J. L. Puget, F. W. Stecker and J. H. Bredekamp, Astrophys. J. **205**, 638 (1976); L. N. Epele and E. Roulet, Phys. Rev. Lett. **81**, 3295 (1998) [arXiv:astro-ph/9806251]; L. N. Epele and E. Roulet, JHEP **9810**, 009 (1998) [arXiv:astro-ph/9808104]; F. W. Stecker, Phys. Rev. Lett. **81**, 3296 (1998); F. W. Stecker and M. H. Salamon, Astrophys. J. **512**, 521 (1992) [arXiv:astro-ph/9808110].
12. D. R. Bergman, Proc. 28th International Cosmic Ray Conference, Tsukuba, Japan, **1**, 397 (2003); see http://www-rccn.icrr.u-tokyo.ac.jp/icrc2003/PROCEEDINGS/HDFA100cpdf**19-eV with modifications by the galactic magnetic Astrophys. J. **596**, 1044 (2003) [arXiv:astro-ph/0307038].
13. for reviews see, e.g., P. P. Kronberg, Rept. Prog. Phys. **57**, 325 (1994); D. Grasso and H. R. Rubinstein, Phys. Rept. **348**, 163 (2001) [arXiv:astro-ph/0009061].
14. J. P. Vallée, Fundamentals of Cosmic Physics **19** (1997) 1; J. L. Han and R. Wielebinski, arXiv:astro-ph/0209090.
15. D. Ryu, H. Kang, and P. L. Biermann, Astron. Astrophys. **335** (1998) 19.
16. G. A. Medina-Tanco and T. A. Ensslin, Astropart. Phys. **16**, 47 (2001) [arXiv:astro-ph/0011454].
17. E. Waxman and J. Miralda-Escude, Astrophys. J. **472**, L89 (1996) [arXiv:astro-ph/9607059].
18. T. Stanev, arXiv:astro-ph/0303123; T. Stanev, D. Seckel and R. Engel, Phys. Rev. D **68**, 103004 (2003) [arXiv:astro-ph/0108338]; T. Stanev, R. Engel, A. Mucke, R. J. Protheroe and J. P. Rachen, Phys. Rev. D **62**, 093005 (2000) [arXiv:astro-ph/0003484].
19. O. Deligny, A. Letessier-Selvon and E. Parizot, arXiv:astro-ph/0303624.
20. G. Sigl, M. Lemoine and P. Biermann, Astropart. Phys. **10**, 141 (1999) [arXiv:astro-ph/9806283].
21. C. Isola, M. Lemoine and G. Sigl, Phys. Rev. D **65**, 023004 (2002) [arXiv:astro-ph/0104289].
22. M. Lemoine, G. Sigl and P. Biermann, arXiv:astro-ph/9903124.
23. C. Isola and G. Sigl, Phys. Rev. D **66**, 083002 (2002) [arXiv:astro-ph/0203273].
24. P. Sommers, Astropart. Phys. **14**, 271 (2001) [arXiv:astro-ph/0004016].
25. P. Blasi and D. De Marco, Astropart. Phys. **20**, 559 (2004) [arXiv:astro-ph/0307067].
26. P. Blasi and A. V. Olinto, Phys. Rev. D **59**, 023001 (1999) [arXiv:astro-ph/9806264].
27. H. Yoshiguchi, S. Nagataki, S. Tsubaki and K. Sato, Astrophys. J. **586**, 1211 (2003) [Erratum-ibid. **601**, 592 (2004)] [arXiv:astro-ph/0210132]; H. Yoshiguchi, S. Nagataki and K. Sato, http://www-rccn.icrr.u-tokyo.ac.jp/icrc2003/PROCEEDINGS/HDFA100cpdf**19-eV with modifications by the galactic magnetic Astrophys. J. **596**, 1044 (2003) [arXiv:astro-ph/0307038].
28. R. Aloisio and V. Berezinsky, arXiv:astro-ph/0403095.
29. G. Medina Tanco, “Cosmic magnetic fields from the perspective of ultra-high-energy cosmic rays propagation”, Lect. Notes Phys. **576** (2001) 155.
30. G. Sigl, F. Miniati and T. A. Ensslin, Phys. Rev. D **68**, 043002 (2003) [arXiv:astro-ph/0302388]; G. Sigl, F. Miniati and T. A. Ensslin, arXiv:astro-ph/0309695; G. Sigl, F. Miniati and T. A. Ensslin, Phys. Rev. D **70**, 043007 (2004) [arXiv:astro-ph/0401084].
31. K. Dolag, D. Grasso, V. Springel and I. Tkachev, JETP. Lett. **79**, 583 (2004) [arXiv:astro-ph/0310902].
32. R. M. Kulsrud, R. Cen, J. P. Ostriker and D. Ryu, Astrophys. J. **480** (1997) 481.
33. K. Dolag, D. Grasso, V. Springel, and I. Tkachev, these proceedings of the “Cosmic Ray International Seminar: GZK and Surroundings”, Catania, May 31 - June 4, 2004.
34. E. Armengaud, F. Miniati, G. Sigl et al., in preparation.
35. see, e.g., A. A. Watson, arXiv:astro-ph/0312475, and ref-

erences therein; A. A. Watson, arXiv:astro-ph/0408110.

36. G. Bertone, C. Isola, M. Lemoine and G. Sigl, Phys. Rev. D **66**, 103003 (2002) [arXiv:astro-ph/0209192].
37. see, e.g., L. N. Epele and E. Roulet, JHEP **9810**, 009 (1998) [arXiv:astro-ph/9808104].
38. T. Yamamoto, K. Mase, M. Takeda, N. Sakaki and M. Teshima, Astropart. Phys. **20**, 405 (2004) [arXiv:astro-ph/0312275].
39. G. Sigl, JCAP **08**, 012 (2004) [arXiv:astro-ph/0405549].
40. T. Wibig and A. W. Wolfendale, arXiv:astro-ph/0406511.
41. M. Takeda *et al.*, Phys. Rev. Lett. **81**, 1163 (1998) [arXiv:astro-ph/9807193]; M. Takeda *et al.*, Astrophys. J. **522**, 225 (1999) [arXiv:astro-ph/9902239]; N. Hayashida *et al.*, arXiv:astro-ph/0008102; see also <http://www-akeno.icrr.u-tokyo.ac.jp/AGASA/>.
42. T. Abu-Zayyad *et al.* [High Resolution Fly's Eye Collaboration], arXiv:astro-ph/0208243; T. Abu-Zayyad *et al.* [High Resolution Fly's Eye Collaboration], arXiv:astro-ph/0208301.
43. L. Anchordoqui, H. Goldberg, S. Reucroft and J. Swain, Phys. Rev. D **64**, 123004 (2001) [arXiv:hep-ph/0107287].